JACS
JOURNAL OF THE AMERICAN CHEMICAL SOCIETY
Article
pubs.acs.org/JACS

Highly Coplanar Very Long Oligo(alkylfuran)s: A Conjugated System with Specific Head-To-Head Defect

Xu-Hui Jin,* Dennis Sheberla,† Linda J. W. Shimon, and Michael Bendikov‡

Department of Organic Chemistry and Chemical Research Support Unit, Weizmann Institute of Science, Rehovot 76100, Israel

Supporting Information

ABSTRACT: Well-defined monodisperse conjugated oligomers, which have planar backbones and are free from the disturbance of substituents, attract broad interest. Herein, we report a series of symmetrical, isomerically pure oligofurans, namely, the 16-mer **16F-6C$_6$** together with the related ***n*F-2C$_6$** (n = 4, 6, 8). Through computational studies and detailed spectroscopic and X-ray characterization, for the first time, we show that the planarity of the furan backbone is almost unaffected by the head-to-head defect which is known to cause considerable twists in its oligo- or polythiophene analogues. We present that the properties of these rigid oligo(alkylfuran)s are strongly influenced by the conjugation length. As the longest monodisperse α-oligofuran synthesized to date, **16F-6C$_6$** was observed to be stable and highly fluorescent. Experimental and computational studies of the redox states of these oligo(alkylfuran)s reveal that **16F-6C$_6$** has singlet biradical (polaron-pair) character in the doubly oxidized ground state: the open-shell singlet ($\langle S_2 \rangle$ = 0.989) is 3.8 kcal/mol more stable than the closed-shell dication.

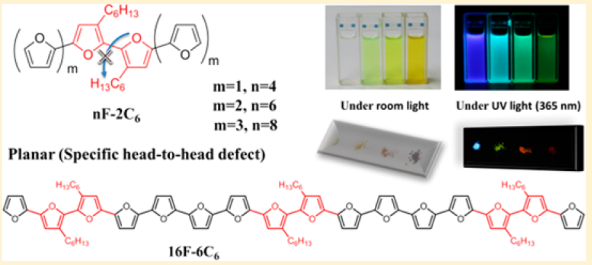

INTRODUCTION

Conjugated oligomers and polymers have attracted considerable attention because of their broad potential in optoelectronic devices, including organic light-emitting diodes (OLEDs),[1] organic field-effect transistors (OFETs),[2] and solar cells.[3] One major concern regarding the organic semiconductor materials is the planarity of their π-conjugated backbones because a highly planar molecular conformation can promote good electronic delocalization, minimized band gaps, and close solid-state $\pi-\pi$ stacking, which are altogether required in real applications.[4] Although long oligo- and polythiophenes are the most widely used and best-studied conjugated material to date, preserving the backbone planarity of these extended conjugated systems remains a challenge.[5] The major reason is that extended thiophene-based materials generally require backbone functionalization to improve their poor solubilities and processability, and these substituents can easily cause twisting of their backbone due to the low twisting potential of thiophene rings.[5b,6] One well-known characteristic is that the planarity of thiophene-based materials significantly depends on the linkage of the thiophene units: when the adjacent alkyl substituents are located in a symmetric head-to-head fashion (3,3′-substitution), the thiophene rings are found to become considerably nonplanar due to a large intrachain steric effect.[7] For this reason, symmetrical disubstituted thiophene monomers, except for EDOT,[8] have not yielded useful polythiophenes to date. Regulating alkyl substituents in the head-to-tail (HT) position (3,4′-substitution) can promote the planarity of polythiophenes; a prominent example is the most widely investigated poly(3-hexylthiophene) (P3HT).[5a,9] However, this typically requires costly and complex regioselective syntheses because the 3-alkylthiophene monomers are asymmetric and the head-to-head coupling may occur during their polymerization in a nonregiospecific fashion. The same problem also exists in the synthesis of planar regioregular monodisperse oligo(3-alkylthiophene)s. Although a number of routes, such as metal-catalyzed cross-coupling methodologies, have been used for the development of high-purity long oligo(3-alkylthiophene)s over the years,[5b,10] only very recently have pure monodisperse regioregular oligo(3-hexylthiophene)s up to 36 repeating units been successfully developed and studied.[11,12]

α-Oligofurans, which were recently disclosed by our group, are close oligothiophene analogues that exhibit higher fluorescence, better solubility, greater rigidity, and tighter solid-state packing than the corresponding oligothiophenes.[13] A computational study indicates that long oligofurans exhibit a greater quinoid character and lower ionization energies (because of the higher energy of their HOMO) than the corresponding oligothiophenes.[14] These computational results are in agreement with experimental observations with respect to their extensive conjugation[15] and good charge delocalization along the oligofuran backbone.[16] Our recent device investigation also demonstrated that oligofurans possess the field-effect mobility similar to that of the corresponding oligothiophenes.[17] Therefore, oligofurans could be promising alternatives to oligothiophenes.[18]

Similarly, there is also a rapidly growing interest in other furan-containing materials.[19] An array of furan-containing

Received: November 28, 2013
Published: January 17, 2014

   dx.doi.org/10.1021/ja411842g | J. Am. Chem. Soc. 2014, 136, 2592−2601

oligomers or polymers have been explored and found to exhibit efficient semiconducting properties in solar cells and OFET applications.[20−22] The furan building blocks have been shown to exhibit significant advantages in contrast with their corresponding thiophene units. For instance, insertion of furan moieties into the backbones of other conjugated polymers was shown to improve considerably the solubility of the polymer in common solvents.[20] Similar results were also observed for short furan-thiophene oligomers. A bifuran capped at each end with a thiophene moiety exhibits entirely different properties from those of a bithiophene with furan caps: the bifuran core bestows on the compound greater rigidity, increased fluorescence, and improved solubility.[23]

Indeed, a growing body of literature suggests the great potential for applications using oligofurans and furan-containing materials; however, several crucial properties are still not known about long furan-based materials. For example, DFT calculations show that the twisting potential of unsubstituted oligofurans is greater than that of the corresponding oligothiophenes,[14] but the influence of substituents on the planarity of long oligofurans is still not clear. Moreover, the structure−property relationships of long oligofurans have also not been understood. We expect that the thorough examination of these properties is especially important as it will offer a clear understanding of the long furan-based materials as an alternative conjugated system for organic electronics.

Herein, we report the synthesis and characterization of a series of symmetrical alkyl-substituted α-oligofurans, namely, the 16-mer **16F-6C$_6$** together with the related ***n*F-2C$_6$** (n = 4, 6, 8). We demonstrate that the planarity of long oligofurans is almost unaffected by the head-to-head defect, which is well-known to cause serious twisting in their oligo- or polythiophene analogues. This is particularly important because it suggests that planar disubstituted furan monomers could serve as useful building blocks for long furan-based materials. In addition, we also show the investigation of basic structure−property relationships of the long oligo(alkylfuran)s, offering fundamental understanding of the connection between conjugation length and various properties, such as absorption, fluorescence, thermal properties, and the nature of charge carriers. It is known that precisely defined long oligomers have often provided relevant insights into related properties of their polymeric materials.[12,24] Therefore, the **16F-6C$_6$**—being the longest monodisperse α-oligofuran synthesized to date—can also be considered a model for the corresponding polyfuran analogues.

RESULTS AND DISCUSSION

Synthesis. The synthesis of oligofurans ***n*F-2C$_6$** (n = 4, 6, 8) is shown in Scheme 1. Bifuran **2F-2C$_6$** was obtained by coupling 3-bromofuran with lithium diisopropylamide (LDA) and $CuCl_2$, followed by a Kumada coupling with hexylmagnesium bromide using catalytic Ni(dppp)Cl_2 (dppp =1,3-bis(diphenylphosphino)propane). Treatment of **2F-2C$_6$** with *N*-bromosuccinimide (NBS) generated dibromide **2**. Whereas stannane **3** is commercially available, stannanes **4** and **5** were prepared according to a previously described method.[13] Stille coupling between dibromide **2** and each of the stannanes (**3**, **4**, and **5**) yielded oligo(alkylfuran)s ***n*F-2C$_6$** (n = 4, 6, and 8, respectively).

Dibromooligofuran **7** was produced by brominating **8F-2C$_6$** with NBS, while tributyltin oligofuran **6** was obtained through

Scheme 1. Synthesis of Long Oligo(alkylfuran)s *n*F-2C$_6$ (n = 4, 6, 8)

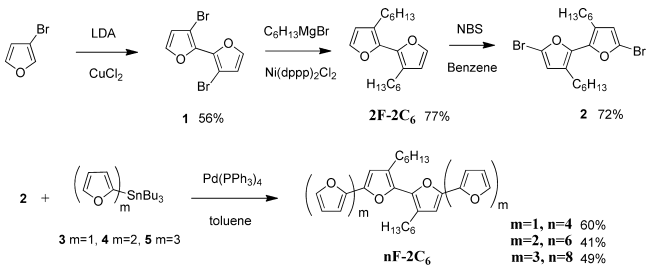

the lithiation of **4F-2C$_6$** with *n*-butyllithium followed by the addition of tributyltin chloride. A one-step Stille coupling reaction of **6** and **7** formed isomerically pure **16F-6C$_6$**; this is the longest known oligofuran to date, with a 5.6 nm backbone (Scheme 2). All synthesized oligo(alkylfuran)s exhibit excellent solubility in common organic solvents, such as toluene, chloroform, DCM, and THF. They have been fully characterized by ^{1}H and ^{13}C NMR spectroscopy and high-resolution mass spectrometry (HRMS). The purity of **16F-6C$_6$** was further analyzed by the HPLC trace (see Supporting Information). All of the oligomers were studied by UV−vis spectroscopy, fluorescence spectroscopy, cyclic voltammetry (CV), thermogravimetric analysis (TGA), and differential scanning calorimetry (DSC).

Photophysical Properties. The photophysical properties of the series of oligo(alkylfuran)s were measured in 1,4-dioxane solution and are shown in Table 1 and Figure 1. The shorter members of the ***n*F-2C$_6$** (n = 4, 6, 8) series exhibit a slight bathochromic shift (4 nm for **4F-2C$_6$**; 5 nm for **6F-2C$_6$** and **8F-2C$_6$**) in the maximum absorption values relative to those of the unsubstituted oligofurans ***n*F** (n = 4, 6, 8),[13] which reflects that the planarity of the disubstituted interfuran link is also preserved in solution. This is in contrast to the analogous oligo(alkylthiophene)s ***n*T-2C$_6$** (n = 4, 5, 6). Even though the hexyl side chains are located on separated terminal thiophene rings with smaller intrachain steric effect than that in a head-to-head fashion, ***n*T-2C$_6$** (n = 4, 5, 6) exhibits a hypsochromic shift of the absorption maximum of 7−14 nm compared with the unsubstituted oligothiophenes ***n*T** (n = 4, 5, 6).[25] Owing to the extended conjugation, the maximum absorption of **16F-6C$_6$** (451 nm) is observed to be red-shifted by about 22 nm compared with that of **8F-2C$_6$**, but it approaches the λ_{max} of poly(**4F-2C$_6$**) (458 nm).[26]

Plots of the energy of the absorption maximum of the series of oligo(alkylfuran)s against the reciprocal number of monomer units ($1/n$) are shown in Figure 2. In the short oligomeric ***n*F-2C$_6$** (n = 4, 6, 8), a linear fit is obtained with an equation of E(eV) = 2.41 + 3.82/n. The slope of 3.82 is similar to that of the equivalent curve for unsubstituted oligofurans (slope = 3.88)[13] but larger than that of the corresponding oligo(alkylthiophene)s (slope = 3.14; alkyl chains are located on the backbone in a head-to-tail fashion).[27] This result suggests that conjugation in oligo(alkylfuran)s is similar to that in unsubstituted oligofurans and better than that in the corresponding oligo(alkylthiophenes)s. **16F-6C$_6$** clearly deviates from this linear plot, which is in line with our previous theoretical studies that, for n > 10, the HOMO−LUMO gap no longer follows linear relationship with the number of furan rings.[14] The saturation of π conjugation causes both its experimental and calculated absorption maxima (Supporting

dx.doi.org/10.1021/ja411842g | J. Am. Chem. Soc. 2014, 136, 2592−2601

Scheme 2. Synthesis of 16F-6C$_6$

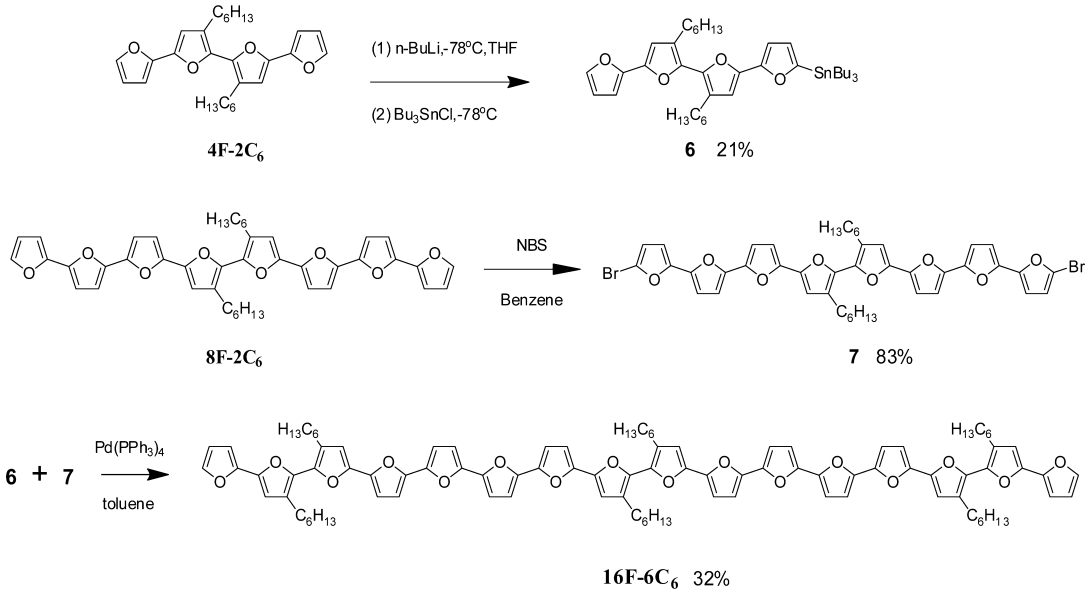

Table 1. Photophysical Data for the Oligo(alkylfuran)s and Unsubstituted Oligofurans *n*F (n = 4–8)[13]

	λ_{abs}[a] (nm)	ε_{max}[a] (M^{-1} cm^{-1})	λ_{flu}[a] (nm)	Φ_f[a]	Stokes shift[a] (eV)	τ_F[a] (ns)	k_F[b] (ns^{-1})	k_{NR}[c] (ns^{-1})	$\lambda_{abs\text{-}calc}$[d] (nm)	f_{abs}[d,e]	$\lambda_{flu\text{-}calc}$[d] (nm)	f_{em}[d,f]	$\lambda_{abs\text{-}film}$[g] (nm)	$\lambda_{flu\text{-}film}$[g] (nm)	Φ_f[h] (solid state)
4F-2C$_6$	368	27400	402, 428	0.82	0.28	1.46	0.56	0.12	395	1.06	402	1.13			0.29
6F-2C$_6$	409	52000	450, 480	0.62	0.28	1.38	0.45	0.28	466	1.76	450	1.91	415	525	0.20
8F-2C$_6$	428	56200	473, 505	0.53	0.27	1.26	0.42	0.37	512	2.37	473	2.59	449	568	0.02
16F-6C$_6$	451	124000	499, 534	0.42	0.27	1.30	0.32	0.45	591	4.80	499	4.97	471	615	<0.01
4F	364	28600	391, 413	0.80	0.25	1.45	0.55	0.14	383	1.21	431	1.29			0.09
5F	388	51000	421, 449	0.74	0.25	1.39	0.53	0.19	423	1.53	476	1.66			0.05
6F	404	53000	442, 472	0.69	0.26	1.31	0.53	0.24	454	1.85	515	2.02			0.05
7F	417	56000	455, 485	0.67	0.25	1.22	0.55	0.27	480	2.15	547	2.35			<0.01
8F	423	56000	467, 499	0.66	0.27	1.30	0.51	0.26	500	2.45	573	2.67			<0.01

[a]Absorbance, absorption maxima, fluorescent spectral maxima, fluorescence quantum yield, and fluorescence lifetime measured in 1,4-dioxane. [b]Calculated according to the equation: $k_F = \Phi_F/\tau_F$. [c]Calculated according to the equation: $\Phi_F = k_F/(k_F + k_{NR})$. [d]Calculated values at TD-B3LYP/6-31G(d).[30] [e]Calculated oscillator strength for absorption. [f]Calculated oscillator strength for fluorescence. [g]Measured in spin-coated thin films prepared using tetrahydrofuran solution. [h]Solid-state quantum yield measured in powder.

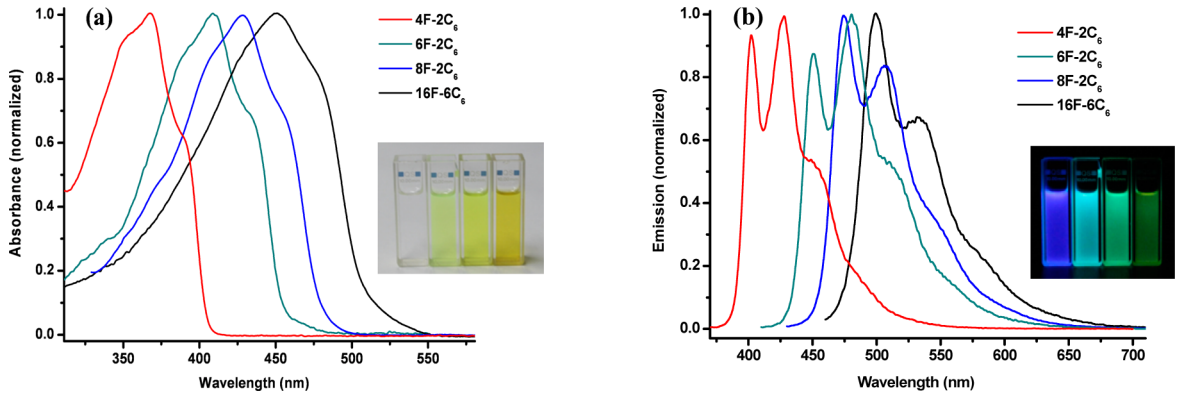

Figure 1. Normalized absorption (a) and emission (b) spectra of ***n*F-2C$_6$** (n = 4, 6, 8) and **16F-6C$_6$** in 1,4-dioxane. Inset: Photographs (from left to right: **4F-2C$_6$**, **6F-2C$_6$**, **8F-2C$_6$**, **16F-6C$_6$**) (a) under ambient light and (b) UV light at a wavelength of 365 nm.

dx.doi.org/10.1021/ja411842g | J. Am. Chem. Soc. 2014, 136, 2592–2601

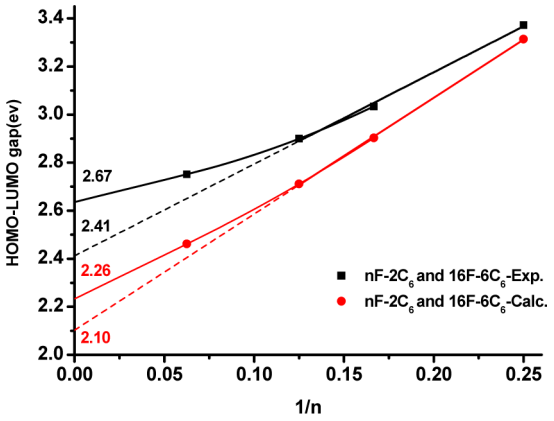

Figure 2. Plot of the calculated [B3LYP/6-31G(d)] (red) and experimental (black) energies of the HOMO−LUMO gaps of ***n*F-2C$_6$** (n = 4, 6, 8) and **16F-6C$_6$** against the reciprocal of the number of monomer units ($1/n$). The linear fits are drawn by including only ***n*F-2C$_6$** (n = 4, 6, 8). Nonlinear fits are drawn by including ***n*F-2C$_6$** (n = 6, 8) and **16F-6C$_6$** using second-order polynomials.

Information Table S1) to be shifted to higher energy values than expected, based on the linear convergence of the values obtained for the ***n*F-2C$_6$** series.[28] Using the second-order polynomial equation from the oligomer data,[29] the band gap of poly(oligo(alkylfuran)) is extrapolated to be 2.67 eV (based on experimental absorption maxima) or 2.26 eV (using the DFT-calculated values [B3LYP/6-31G(d)], Figure 2), respectively.

In order to further understand the influence of alkyl substituents on the planarity of oligofurans, the energies required to twist the conjugated backbone of oligo(alkylfuran)s were calculated and compared with those of the corresponding oligo(alkylthiophene)s. For example, twisting **4F-2C$_6$** to a 30° twist angle requires 3.8 kcal/mol, which is slightly smaller than 5.3 kcal/mol for twisting unsubstituted **4F** to 30° but much larger than the energy of 0.7 kcal/mol for the same angle twist of unsubstituted **4T** (Figure 3a). In contrast, there is a distinct difference in the case of disubstituted oligo(alkylthiophene)s. The total energy of **4T-2C$_6$** with 30° twist angle is observed to be smaller than that of its planar conformer (~2.1 kcal/mol). The decreased twist potential with the increasing twist angle (from 0 to 40°) is indicative of a strong head-to-head defect on the planarity of **4T-2C$_6$**. Twisting **16F-6C$_6$** to a 20° twist angle requires 7.4 kcal/mol. Such a large twisting energy reveals that it is difficult to twist the backbone of **16F-6C$_6$**, although it is functionalized by more hexyl substituents than **4F-2C$_6$**. **16T-6C$_6$** exhibits a similar decreased twist potential (twist angle increases from 0 to 25°) with **4T-2C$_6$** (Figure 3b). The total energy of **16T-6C$_6$** with a 25° twist angle is about 2.5 kcal/mol lower than that of its planar conformer, suggesting that the thiophene rings of **16T-6C$_6$** are twisted in its ground state.

All compounds of ***n*F-2C$_6$** (n = 4, 6, 8) exhibit strong fluorescence, with quantum yields of 53−82%, which are comparable with those of ***n*F** (n = 4, 6, 8) (Table 2). Thus, no fast nonradiative decay of luminescence is introduced by the hexyl substituents. The quantum yield of oligo(alkylfuran)s decreases with the increasing number of furan rings. Interestingly, **16F-6C$_6$** is still highly fluorescent with quantum yields of 42%. The k_{NR} (nonradiative rate constant) value of oligo(alkylfuran)s progressively increases from 0.12 for **4F-2C$_6$** to 0.45 for **16F-6C$_6$**. It is known that intersystem crossing is an important decay pathway for oligothiophenes, but the k_{ISC} of oligofurans was observed to be much smaller than that of the

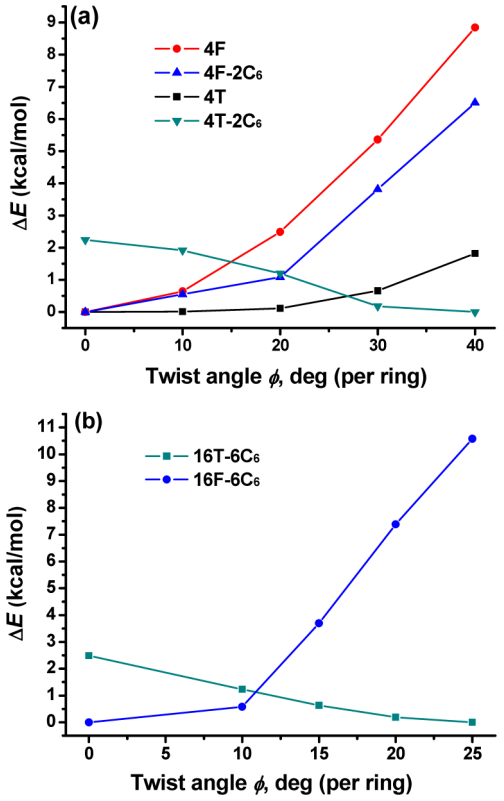

Figure 3. Total twisting energy versus inter-ring twist angle (Φ) for (a) tetrafuran (**4F**), tetrathiophene (**4T**), 3″,4′-dihexyl-2,2′:5′,-2″:5″,2‴-tetrafuran (**4F-2C$_6$**), and 3″,4′-dihexyl-2,2′:5′,2″:5″,2‴-tetrafuran (**4T-2C$_6$**), (b) **16F-6C$_6$**, and **16T-6C$_6$**.

Table 2. Calculated HOMO and LUMO Energy and HOMO−LUMO Gap of *n*F (n = 4, 6, 8) and *n*F-2C$_6$ (n = 4, 6, 8)

	HOMO[a] (eV)	LUMO[a] (eV)	HLG[a,b]
4F-2C$_6$	−4.50	−1.19	3.31
6F-2C$_6$	−4.38	−1.47	2.90
8F-2C$_6$	−4.33	−1.62	2.71
16F-6C$_6$	−4.23	−1.77	2.46
4F	−4.73	−1.30	3.43
6F	−4.55	−1.55	3.00
8F	−4.48	−1.67	2.81

[a]Calculated at the B3LYP/6-31G(d) level. [b]HOMO−LUMO gap.

corresponding oligothiophenes due to the absence of heavy sulfur atoms; that is, the k_{ISC} values of ***n*F** (n = 1−4) are about 10- to 25-fold smaller than for the ***n*T** set.[31] Therefore, the k_{ISC} of oligofurans is essentially negligible compared to oligothiophenes, and the increasing k_{NR} is probably due to the increased degree of molecular freedom with the increasing conjugated chain length.

The Stokes shift values of the ***n*F-2C$_6$** series are 0.27−0.28 eV, which is only slightly higher than the 0.25 eV shift found in unsubstituted oligofurans but much smaller than that of unsubstituted oligothiophenes **3T−6T** (~0.40 eV) and oligo(alkylthiophene)s ***n*T-2C$_6$** (n = 4, 5, 6) (0.45−0.56 eV).[25] This is also consistent with our hypothesis that the alkyl side chains have little effect on the rigidity of the long oligofurans and, unlike in oligothiophenes, they cause no additional reorganization in the excited state.

dx.doi.org/10.1021/ja411842g | J. Am. Chem. Soc. 2014, 136, 2592−2601

Structural Analysis. Single crystals of **6F-2C$_6$** suitable for X-ray crystallography were obtained by recrystallization from dimethyl sulfoxide (DMSO). The analysis indicates that there are two crystallographically independent molecules in each asymmetric unit (Figure 4). The two molecules exhibit almost

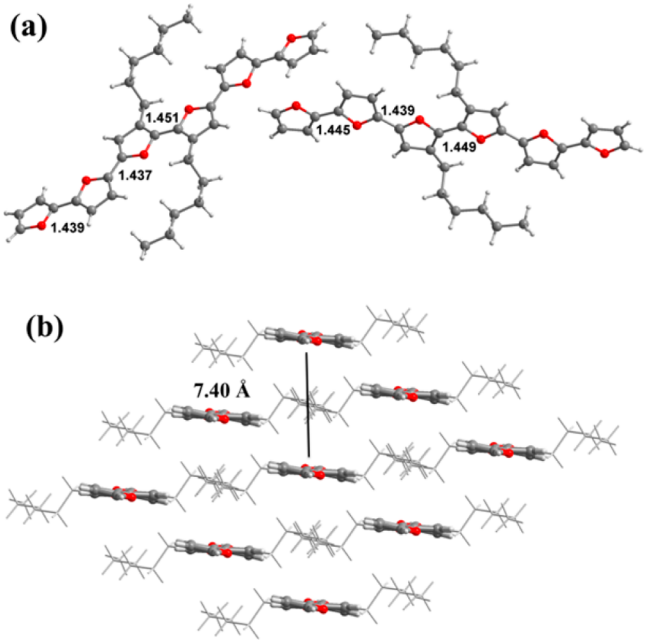

Figure 4. (a) X-ray single-crystal structures of **6F-2C$_6$**. The values represent C−C bond length between the furan rings. (b) Molecular packing of **6F-2C$_6$**. The distance between parallel **6F-2C$_6$** molecules is 7.40 Å.

the same planar configurations with a high degree of conjugation. This is similar to unsubstituted **6F**,[13] which also has a planar structure, but strikingly different from that of 4″,3‴-dimethylsexithiophene (**6T-2C**) which exhibits a larger dihedral angle (26°) between the substituted thiophene ring.[32] Examination of bond lengths in **6F-2C$_6$** indicates that the substitution has only a very small effect on the bond length (elongating the inter-ring C−C bond length by ∼0.01 Å) and exobond C−C−C angles which are increased at the substituted moieties by ∼2°. As most often observed for other planar conjugated structures (including unsubstituted **6F**), **6F-2C$_6$** molecules also pack in a herringbone arrangement (Figure S2). However, as expected, the alkyl chains sterically isolate **6F-2C$_6$** molecules within the herringbone packing arrangement,and consequently, interplane distance of **6F-2C$_6$** is much larger than that of **6F**. This expanded structure, in which no direct $\pi-\pi$ interaction occurs and features large interplanar distances, is expected to suppress the fluorescence quenching and increase solid-state emissions.

Fluorescence in Solid State and Thin Film. Corresponding with the steric effect of hexyl chains and large interplanar distances in solid states, the oligo(alkylfuran)s are observed to exhibit strong solid-state fluorescence, much higher than that of their corresponding unsubstituted oligofurans ***n*F** (n = 4, 6, 8), in which the quantum yield of **4F-2C$_6$** is nearly 3 times greater than that of **4F** (9%). Although the solid-state quantum yield also decreases with increasing chain length, **4F-2C$_6$** and **6F-2C$_6$** still exhibit moderate quantum yields of 29 and 20%.

In thin films, the absorption spectra of ***n*F-2C$_6$** (n = 6, 8) and **16F-6C$_6$** (Figure 5a) are generally characterized by fine vibronic structures, similar to those observed in solution. However, their fluorescence spectra are found featureless, unlike those observed in solutions with the mirror-like peaks (Table 1 and Figure 5b). This result may indicate that there is an delocalization of exciton, which corresponds with Stokes shift values (0.63 for **6F-2C$_6$**, 0.58 for **8F-2C$_6$**, and 0.62 for **16F-6C$_6$** in film) that are larger than those of solutions (0.28 for **6F-2C$_6$**, 0.27 for **8F-2C$_6$**, and 0.27 for **16F-6C$_6$**).

Thermal Properties. The stability of the series of oligo(alkylfuran)s was verified by TGA measurement (Figure S1, Supporting Information). Each compound is found to be stable, and even **16F-6C$_6$** is stable over 180 °C on the basis of the onset of the TGA curve. From DSC analysis, we observed that the melting points of ***n*F-2C$_6$** (n = 4, 6, 8) rise with increasing chain length: **4F-2C$_6$** (32 °C) < **6F-2C$_6$** (119 °C) < **8F-2C$_6$** (135 °C) (Figure 6). These melting points are much lower than those for unsubstituted oligofurans (258 °C for **6F** and 325 °C for **8F**). In contrast with the strong, sharp DSC peaks for ***n*F-2C$_6$** (n = 4, 6, 8), **16F-6C$_6$** was found to exhibit weak, broad peaks at 133.8 and 80.9 °C. A similar behavior is often observed in crystalline polymers.[33] Thus, one can conclude that **16F-6C$_6$** exhibits a lower degree of crystallinity that is closer to those of polymers than to the shorter oligomers.

Cation Radicals of Oligo(alkylfuran)s. The properties of cationic species reveal fundamental aspects of the nature of charge carriers in conjugated organic semiconducting materials.[34] In this respect, long oligofurans have not been investigated. To gain insight into the stability and spectra of the cation radicals of long oligofurans, chemical oxidation of the series of ***n*F-2C$_6$** (n = 4, 6, 8) and **16F-6C$_6$** was studied in CH_2Cl_2 using $(BrC_6H_4)_3NSbCl_6$ as the oxidant. For each

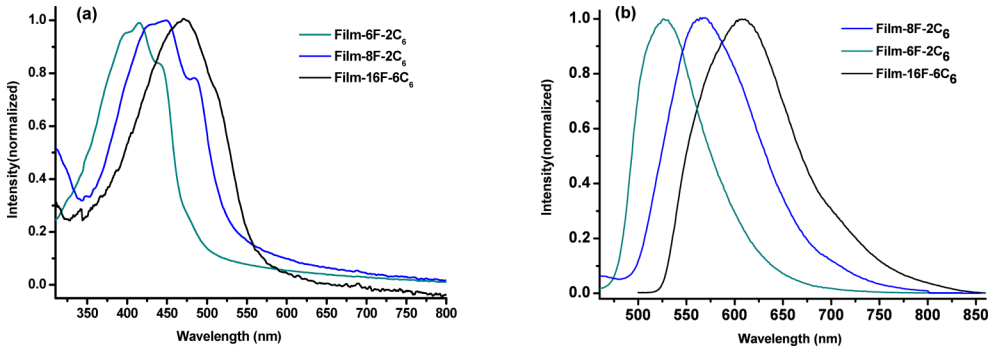

Figure 5. Normalized absorption (a) and emission (b) spectra of **6F-2C$_6$**, **8F-2C$_6$**, and **16F-6C$_6$** as thin films.

dx.doi.org/10.1021/ja411842g | J. Am. Chem. Soc. 2014, 136, 2592−2601

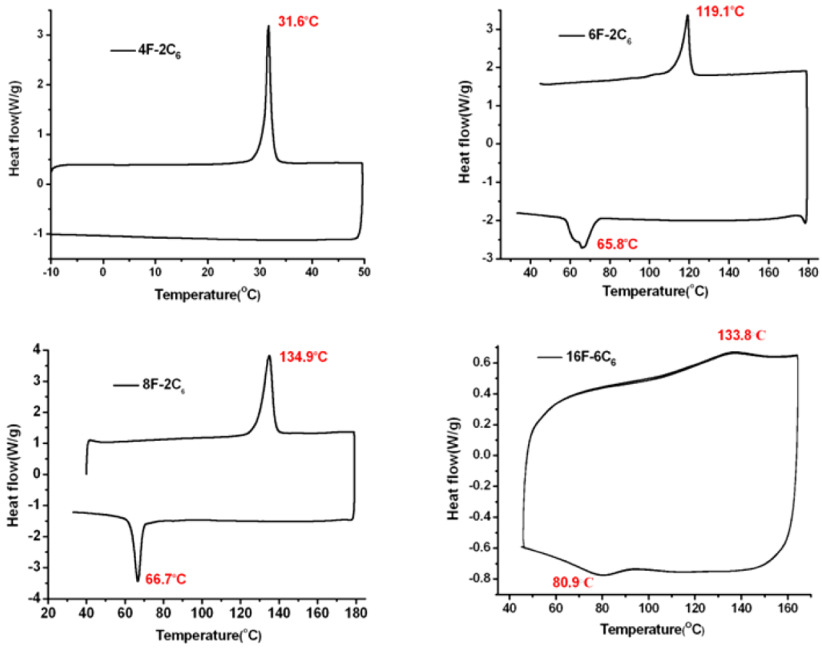

Figure 6. Differential scanning calorimetry (DSC) of ***n*F-2C$_6$** (n = 4, 6, 8) and **16F-6C$_6$** under N_2, rate = 10 °C/min.

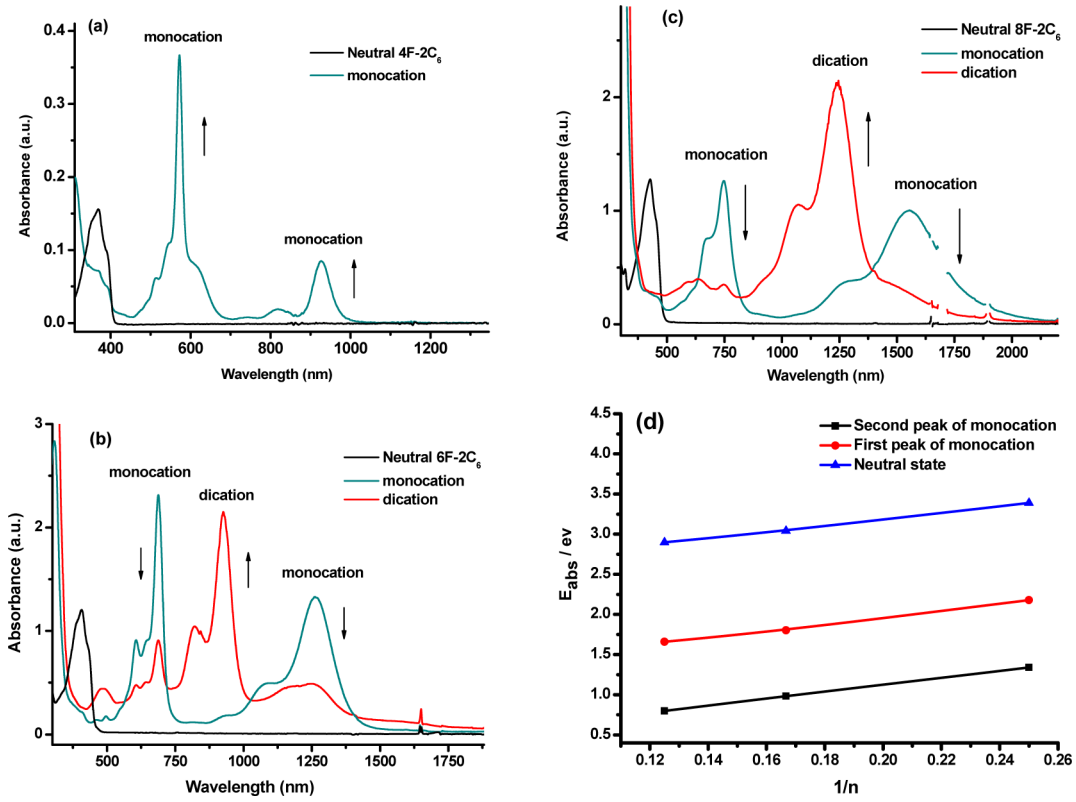

Figure 7. Absorptions in CH_2Cl_2 of ***n*F-2C$_6$** (n = 4, 6, 8) as a neutral molecule and, following oxidation with $(BrC_6H_4)_3NSbCl_6$, as a monocation and dication: (a) **4F-2C$_6$**, (b) **6F-2C$_6$**, and (c) **8F-2C$_6$**. (d) Plots of the energy of the absorption maxima for ***n*F-2C$_6$** (n = 4, 6, 8) in the neutral state and as a monocation against the reciprocal of the number of monomer units ($1/n$).

compound, we observed that their cation radicals were stable during the course of the oxidation experiment. Their absorption spectra in the neutral states are in correspondence with their reduced spectra, which were obtained by adding hydrazine as a reducing agent into solutions of the radical cations (Figure S4 and Figure 8).

The absorption spectra for ***n*F-2C$_6^+$** (n = 4, 6, 8) and ***n*F-2C$_6^{2+}$** (n = 6, 8) are shown in Figure 7. We observed that **4F-2C$_6$** was oxidized to monocation and ***n*F-2C$_6$** (n = 6, 8) was stepwise oxidized up to dications. The energies of the absorption maxima for the neutral molecule, monocation, and dication of ***n*F-2C$_6$** (n = 4, 6, 8) are summarized in Table 3. Figure 7d reveals excellent linear correlations between the

dx.doi.org/10.1021/ja411842g | J. Am. Chem. Soc. 2014, 136, 2592−2601

Table 3. Energy (eV) of Absorption Maxima of *n*F-2C$_6$ (n = 4, 6, 8) in the Neutral State and as Monocations and Dications[a]

absorption band	4F-2C$_6$	6F-2C$_6$	8F-2C$_6$
E_0	3.39 (366)	3.04 (408)	2.90 (427)
$E_{1+}{}^1$	2.18 (569)	1.80 (689)	1.66 (747)
$E_{1+}{}^2$	1.34 (925)	0.98(1265)	0.80 (550)
E_{2+}		1.34 (925)	1.00(1240)

[a] E_0 is the energy (eV) of the absorption maximum in the neutral state. $E_{1+}{}^1$ and $E_{1+}{}^2$ are the energies of the first and second absorption maxima of the monocation. E_{2+} is the energy of the absorption maximum of the dication. Values in parentheses are absorption maxima in nanometers.

absorption energies of ***n*F-2C$_6$** (n = 4, 6, 8) in their neutral state and as a monocation against the reciprocal number of furan rings. Compared with oligo(alkylthiophene)s, which were reported to exhibit similar slopes for the monocation (3.7) and neutral (3.6) species,[35] the slopes for the first (4.19) and second (4.32) peaks of the monocation of ***n*F-2C$_6$** (n = 4, 6, 8) are much steeper than those in their neutral states (3.97), which indicates that the monocations of oligo(alkylfuran)s are better conjugated than their neutral species. This is consistent with the results of computational studies of the unsubstituted oligofurans, which show twisting energies for the cation radicals of α-oligofuran higher than those for their neutral species.[14]

Compared with shorter ***n*F-2C$_6$** (n = 4, 6, 8) series, the **16F-6C$_6$** molecule exhibits completely different behaviors of chemical oxidation under the same conditions. As shown in Figure 8, a small peak at ~710 nm and a large peak at ~2250

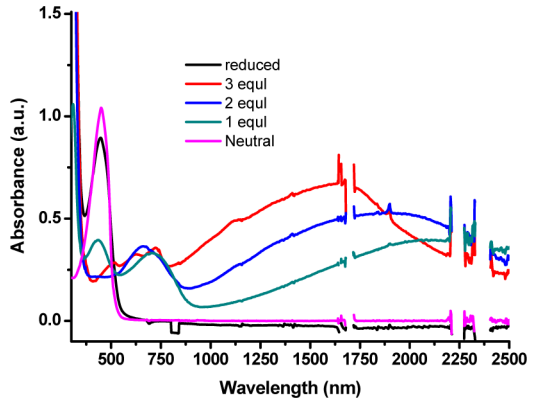

Figure 8. Absorptions of **16F-6C$_6$** in CH_2Cl_2 as a neutral molecule and in various oxidation states obtained using different amounts of $(BrC_6H_4)_3NSbCl_6$ as oxidant. The reduced spectrum was recorded using hydrazine as a reducing agent following oxidation with $(BrC_6H_4)_3NSbCl_6$ in CH_2Cl_2.

nm emerged when it was doped by 1 equiv of the oxidant of $(BrC_6H_4)_3NSbCl_6$ in CH_2Cl_2. Unlike sharp peaks of the radical cations of ***n*F-2C$_6$** (n = 4, 6, 8), the peak at ~2250 nm is found to be broad. Interestingly, as oxidation proceeds with the quantity of oxidant increasing to 3 equiv, the radical cations of **16F-6C$_6$** consistently show two absorption bands in the spectra. Meanwhile, the broad peak at ~2250 nm was observed to blue shift to 1950 nm and finally to 1655 nm in this procedure. This behavior resembles the doping of polymers with a bipolaronic pair and polaronic species.[36] In order to understand this phenomenon, we preformed DFT calculations at UB3LYP/6-31G(d) level accounting for solvation (PCM-(DCM)). The calculation results indicate that the first (4.32 eV) and the second (4.53 eV) ionization potentials (IP) of **16F-6C$_6$** are very close. Thus, pure one-electron oxidation (cation radical) is difficult to achieve experimentally, and even at low oxidant concentration, double oxidation of **16F-6C$_6$** can take place. We have previously shown that ground states of doubly oxidized long oligofurans, oligothiophenes, and oligoselenophenes have a biradical (i.e., polaron-pair) character.[14,37] Similarly, for **16F-6C$_6$**, restricted (RB3LYP) calculations show an instability of the wave function, and broken symmetry unrestricted (BS-UB3LYP) total energy is 3.8 kcal/mol lower than RB3LYP energy, as well spin-contamination value $\langle S_2 \rangle$ = 0.989 is close to theoretical value of 1.000 for singlet biradical state. Additionally, triplet biradical state is only 0.2 kcal/mol higher than the singlet biradical state, meaning that two cation radicals (polarons) are almost noninteracting. Thus **16F-6C$_6$** is long enough to have a large biradical (polaron-pair) contribution to doubly oxidized ground state. TD-DFT calculations of excited states (Table 4) are consistent with the absorption spectra of different oxidation states of **16F-6C$_6$** (Figure 8).

Table 4. Calculated (TD-UB3LYP/6-31G(d)/PCM(DCM)) Excited State Transition Energies and Oscillator Strengths for the Cation Radical and Singlet Biradical of 16F-6C$_6$

	transition 1	transition 2	transition 3
monocation, nm (eV)	3560 (0.35)	807 (1.54)	745 (1.66)
monocation, oscillator strength	1.85	0.90	0.37
dication, nm (eV)	2863 (0.43)	1158 (1.07)	745 (1.66)
dication, oscillator strength	2.79	0.16	2.81

Oxidation Potentials and Electropolymerization. The cyclic voltammetry (CV) traces of ***n*F-2C$_6$** (n = 4, 6, 8) and **16F-6C$_6$** were measured in 1,2-dichloroethane (DCE) with 0.1 M tetra-*n*-butylammonium tetrafluoroborate ($TBABF_4$) as the electrolyte. As shown in Figure 9a, ***n*F-2C$_6$** (n = 4, 6, 8) exhibits reversible oxidation peaks, and in contrast, longer **16F-6C$_6$** shows quasi-reversible oxidation and reduction waves. The oxidation potentials for these oligo(alkylfuran)s are summarized in Table 5. As chain length increases, the first oxidation potential decreases from 0.66 V for **4F-2C$_6$** to 0.41 V for **16F-6C$_6$**, which is in agreement with the increase in the calculated HOMO from −4.50 to −4.23 eV. In accordance with the higher calculated HOMO energies (Table 2) of the oligo(alkylfuran)s compared to their unsubstituted analogues (Table 2), the first oxidation potential of ***n*F-2C$_6$** is lower than that of the corresponding unsubstituted oligofuran by ~0.05−0.08 V.

The electrochemical polymerization of the **16F-6C$_6$** monomer was also studied. A smooth film of poly(**16F-6C$_6$**) was prepared by repeated cyclic voltammetry scans in 1,2-dichloroethane with 0.1 M $TBABF_4$ as the electrolyte, using ITO-coated glass as the electrode. Figure 9b shows the CV traces recorded between −0.2 and 0.8 V vs Ag/AgCl during generation of the film. After near 60 cycles, a thin orange film was produced on the surface of the ITO glass. This thin film did not dissolve in common organic solvents, such as hexane, dichloromethane, methanol, and toluene. The topography of the surface of the film was examined by atomic force microscopy (AFM), which indicated that the film completely covered the electrode with low root mean squared (rms)

dx.doi.org/10.1021/ja411842g | J. Am. Chem. Soc. 2014, 136, 2592−2601

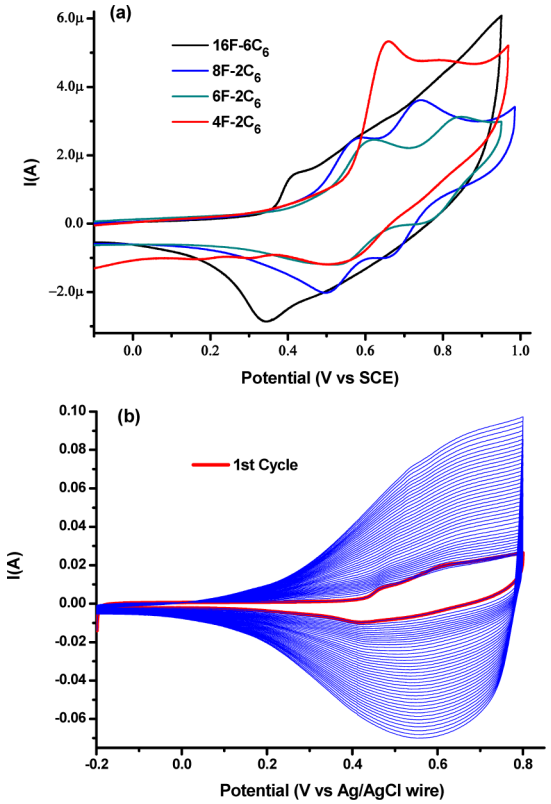

Figure 9. (a) CV of ***n*F-2C$_6$** (n = 4, 6, 8) and **16F-6C$_6$** measured in DCE with 0.1 M $TBABF_4$ (scan rate 50 mV/s) vs Ag/AgCl wire calibrated using Fc/Fc+ (Fc/Fc+ = 0.40 V vs SCE). (b) Repetitive CV scans of **16F-6C$_6$** DCE with 0.1 M $TBABF_4$ (scan rate 50 mV/s).

Table 5. Oxidation Potentials of *n*F-2C$_6$ (n = 4, 6, 8) and 16F-6C$_6$[a]

oxidation potential (vs SCE)	4F-2C$_6$	6F-2C$_6$	8F-2C$_6$	16F-6C$_6$[d]
E_{ox}[b]	0.66	0.61	0.57	0.41
$E_{1/2(ox)}$[c]	0.58	0.56	0.52	

[a]Oxidation potentials were measured vs Ag/AgCl wire in 1,2-dichloroethane (DCE) with 0.1 M $TBABF_4$ at a scan rate of 50 mV/s (all data were calibrated using Fc/Fc+, Fc/Fc+ = 0.40 V vs SCE with DCE as solvent[38]). [b]E_{ox} is taken as the maximum of the first oxidation peak. [c]$E_{1/2(ox)}$ presents the half-wave potential. [d]$E_{1/2(ox)}$ value of **16F-6C$_6$** was not provided because **16F-6C$_6$** was electropolymerized during the procedure of CV measurement.

roughness of 8.6 nm for 3.5 × 3.5 μm and 5.8 nm for 500 × 500 nm square (rms roughness of ITO clean glass is about 4−5 nm) (Figure S5).

Spectroelectrochemical data for the poly(**16F-6C$_6$**) film that formed on the ITO electrode are shown in Figure 10. A characteristic absorption band at λ_{max} = 479 nm can be observed in the neutral state at a potential of −0.2 V. Interestingly, this wavelength for the main peak is substantially larger than the λ_{max} of polyfurans (from 456 to 466 nm) that we have previously obtained from shorter monomers using the electrochemical polymerization method.[39] The bathochromic absorption may indicate better conjugation or more efficient intermolecular interactions in poly(**16F-6C$_6$**) that was obtained from the longer **16F-6C$_6$** monomer.

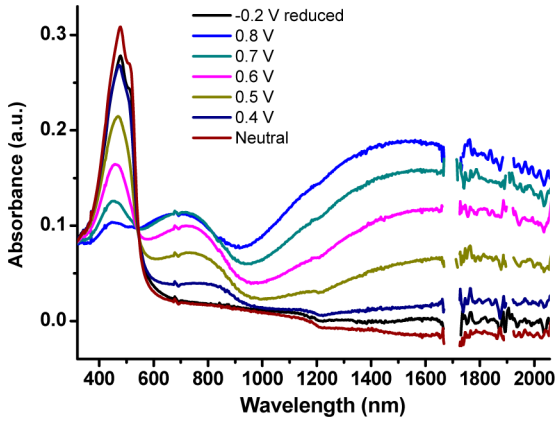

Figure 10. Spectroelectrochemistry of poly(**16F-6C$_6$**) thin film on ITO-coated glass as the potential is scanned between +0.8 and −0.2 V in 1,2-dichloroethane.

CONCLUSIONS

Through step-by-step synthesis, we succeeded in obtaining isomerically pure long oligo(alkylfuran)s possessing well-defined structures up to the 16-mer. Detailed computational studies and spectroscopic and X-ray characterization indicate that alkyl side chains hardly affected the planarity of long oligo(alkylfuran)s. This is distinct from the analogous oligo(alkylthiophene)s and poly(alkylthiophene)s where introduction of two alkyl groups on the neighboring units (via head-to-head connection) causes a significant twist to the conjugated backbone. It suggests that disubstituted furan monomers may serve as useful building blocks for long furan-based materials. Through comparative investigations of the light absorption, fluorescence, thermal properties, spectra of cationic species, oxidation potentials, and electropolymerization, we have shown the key role of the conjugation length on the property variations of oligofurans. As the longest monodisperse α-oligofuran synthesized to date, we present that the rigid **16F-6C$_6$** exhibits properties approaching those of its corresponding polymeric analogues. It is highly fluorescent and possesses singlet biradical (polaron-pair) character in the doubly oxidized ground state.

Overall, this work demonstrates the remarkable backbone planarity of disubstituted oligo(alkylfuran)s. It suggests that, unlike oligothiophenes, the head-to-head coupling is not a limitation of the preparation of planar long furan-based materials. The detailed characterization presents a fundamental understanding of the property variations of rigid long oligofurans with increasing conjugation length.

ASSOCIATED CONTENT

Supporting Information

Detailed synthesis and characterization of ***n*F-2C$_6$** and **16F-6C$_6$**, ^1H and ^{13}CNMR spectra, TGA traces, electrochemistry, optimized structures and total energies of all calculated molecules (B3LYP/6-31G(d)), TD-DFT calculation of UV and fluorescence, FTIR-ATR spectra, AFM analysis of poly(**16F-6C$_6$**) film, CIF file of **6F-2C$_6$**. This material is available free of charge via the Internet at http://pubs.acs.org.

AUTHOR INFORMATION

Corresponding Author

xuhui.jin@weizmann.ac.il

Present Address

[†]Department of Chemistry, Massachusetts Institute of Technology, 77 Massachusetts Avenue, Cambridge, Massachusetts 02139, United States.

Notes

The authors declare no competing financial interest.

[‡]Deceased July 2, 2013.

■ ACKNOWLEDGMENTS

We thank Prof. Dmitrii F. Perepichka (McGill University) for many useful discussions and suggestions to improve this paper. We thank Dr. Sagar Sharma for his helpful discussion about calculations, Dr. Natalia Zamoshchik for her help in AFM analysis, and Dr. Ori Gidron and Erez Cohen for their help in the solid-state fluorescence quantum yield and fluorescence lifetime measurements. We thank the MINERVA Foundation for financial support. M.B. was a member ad personam of the Lise Meitner-Minerva Center for Computational Quantum Chemistry.

■ DEDICATION

In memory of Professor Michael Bendikov.

■ REFERENCES

(1) (a) Reineke, S.; Lindner, F.; Schwartz, G.; Seidler, N.; Walzer, K.; Lueesem, B.; Leo, K. *Nature* **2009**, *459*, 234. (b) Xiao, L.; Chen, Z.; Qu, B.; Luo, J.; Kong, S.; Gong, Q.; Kido, J. *Adv. Mater.* **2011**, *23*, 926.

(2) (a) *Organic Field Effect Transistors*; Bao, Z., Locklin, J., Eds.; CRC Press: Boca Raton, FL, 2007. (b) Wang, C.; Dong, H.; Hu, W.; Liu, Y.; Zhu, D. *Chem. Rev.* **2012**, *112*, 2208. (c) Lee, T.; Landis, C. A.; Dhar, B. M.; Jung, B. J.; Sun, J.; Sarjeant, A.; Lee, H.-J.; Katz, H. E. *J. Am. Chem. Soc.* **2009**, *131*, 1692. (d) Pho, T. V.; Yuen, J. D.; Kurzman, J. A.; Smith, B. G.; Miao, M. S.; Walker, W. T.; Seshadri, R.; Wudl, F. *J. Am. Chem. Soc.* **2012**, *134*, 8185. (e) Mitsui, C.; Soeda, J.; Miwa, K.; Tsuji, H.; Takeya, J.; Nakamura, E. *J. Am. Chem. Soc.* **2012**, *134*, 5448. (f) Shinamura, S.; Osaka, I.; Miyazaki, E.; Nakao, A.; Yamagishi, M.; Takeya, J.; Takimiya, K. *J. Am. Chem. Soc.* **2011**, *133*, 5024. (g) Niimi, K.; Shinamura, S.; Osaka, I.; Miyazaki, E.; Takimiya, K. *J. Am. Chem. Soc.* **2011**, *133*, 8732. (h) Guo, X.; Puniredd, S. R.; Baumgarten, M.; Pisula, W.; Müllen, K. *J. Am. Chem. Soc.* **2012**, *134*, 8404. (i) Wang, S.; Kiersnowski, A.; Pisula, W.; Müllen, K. *J. Am. Chem. Soc.* **2012**, *134*, 4015.

(3) (a) Cheng, Y.-J.; Yang, S.-H.; Hsu, C.-S. *Chem. Rev.* **2009**, *109*, 5868. (b) Haid, S.; Mishral, A.; Weil, M.; Uhrich, C.; Pfeiffer, M.; Bäuerle, P. *Adv. Funct. Mater.* **2012**, *22*, 4322. (c) Zhou, J. Y.; Wan, X. J.; Liu, Y. S.; Zuo, Y.; Li, Z.; He, G. R.; Long, G. K.; Ni, W.; Li, C. X.; Su, X. C.; Chen, Y. S. *J. Am. Chem. Soc.* **2012**, *134*, 16345.

(4) (a) Huang, H.; Chen, Z.; Ortiz, R. P.; Newman, C.; Usta, H.; Lou, S.; Youn, J.; Noh, Y.-Y.; Baeg, K.-J.; Chen, L. X.; Facchetti, A.; Marks, T. *J. Am. Chem. Soc.* **2012**, *134*, 10966. (b) Salleo, A.; Kline, R. J.; DeLongchamp, D. M.; Chabinyc, M. L. *Adv. Mater.* **2010**, *22*, 3812.

(5) (a) *Handbook of Thiophene-Based Materials*; Perepichka, I. F., Perepichka, D. F., Eds.; Wiley-VCH: Weinheim, Germany, 2009. (b) *Hand-Book of Oligo- and Polythiophenes*; Fichou, D., Ed.; Wiley-VCH: Weinheim, Germany, 1999. (c) Mishra, A.; Ma, C. Q.; Bäuerle, P. *Chem. Rev.* **2009**, *109*, 1141.

(6) Zade, S. S.; Bendikov, M. *Chem.—Eur. J.* **2007**, *13*, 3688.

(7) (a) Maior, R. M. S.; Hinkelmann, K.; Eckert, H.; Wudl, F. *Macromolecules* **1990**, *23*, 1268. (b) Gill, R. E.; Malliaras, G. G.; Wildeman, J.; Hadziioannou, G. *Adv. Mater.* **1994**, *6*, 132. (c) Fukunaga, T.; Harada, K.; Takashima, W.; Kaneto, K. *Jpn. J. Appl. Phys.* **1997**, *36*, 4466. (d) Hayashi, N.; Matsuda, A.; Chikamatsu, E.; Mori, K.; Higuchi, H. *Tetrahedron Lett.* **2003**, *44*, 7155.

(8) (a) Groenendaal, L.; Jonas, F.; Freitag, D.; Pielartzik, H.; Reynolds, J. R. *Adv. Mater.* **2000**, *12*, 481. (b) Groenendaal, L.; Zotti, G.; Aubert, P. H.; Waybright, S. M.; Reynolds, J. R. *Adv. Mater.* **2003**, *15*, 855. (c) Roncali, J.; Blanchard, P.; Frere, P. *J. Mater. Chem.* **2005**, *15*, 1589. (d) Kirchmeyer, S.; Reuter, K. *J. Mater. Chem.* **2005**, *15*, 2077.

(9) (a) Perepichka, I. F.; Perepichka, D. F.; Meng, H.; Wudl, F. *Adv. Mater.* **2005**, *17*, 2281. (b) Marrocchi, A.; Lanari, D.; Facchetti, A.; Vaccaro, L. *Energy Environ. Sci.* **2012**, *5*, 8457.

(10) (a) Guillerez, S.; Bidan, G. *Synth. Met.* **1998**, *93*, 123. (b) Kirschbaum, T.; Azumi, R.; Mena-Osteritz, E.; Bäuerle, P. *New J. Chem.* **1999**, *23*, 241.

(11) Koch, F. P. V.; Smith, P.; Heeney, M. *J. Am. Chem. Soc.* **2013**, *135*, 13695.

(12) Koch, F. P. V.; Heeney, M.; Smith, P. *J. Am. Chem. Soc.* **2013**, *135*, 13699.

(13) Gidron, O.; Diskin-Posner, Y.; Bendikov, M. *J. Am. Chem. Soc.* **2010**, *132*, 2148.

(14) Sharma, S.; Bendikov, M. *Chem.—Eur. J.* **2013**, *19*, 13127.

(15) Ferrón, C. C.; Ruiz Delgado, M. C.; Gidron, O.; Sharma, S.; Sheberla, D.; Sheynin, Y.; Bendikov, M.; López Navarrete, J. T.; Hernández, V. *Chem. Commun.* **2012**, *48*, 6732.

(16) Gidron, O.; Diskin-Posner, Y.; Bendikov, M. *Chem.—Eur. J.* **2013**, *19*, 13140.

(17) (a) Gidron, O.; Dadvand, A.; Sheynin, Y.; Bendikov, M.; Perepichka, D. F. *Chem. Commun.* **2011**, *47*, 1976. (b) Gidron, O.; Dadvand, A.; Sun, W.-H.; Chung, I.; Shimon, L.; Bendikov, M.; Perepichka, D. *J. Mater. Chem. C* **2013**, *1*, 4358.

(18) Bunz, U. H. F. *Angew. Chem., Int. Ed.* **2010**, *49*, 5037.

(19) *Encyclopedia of Polymer Science and Technology*; Streifel, B. C., Tovar, J. D., Eds.; Wiley & Sons, Inc.: New York, 2013. DOI: 10.1002/0471440264.pst578.

(20) Woo, C. H.; Beaujuge, P. M.; Holcombe, T. W.; Lee, O. P.; Fréchet, J. M. J. *J. Am. Chem. Soc.* **2010**, *132*, 15547.

(21) Li, Y.; Sonar, P.; Singh, S. P.; Zeng, W.; Soh, M. S. *J. Mater. Chem.* **2011**, *21*, 10829.

(22) Bijleveld, J. C.; Karsten, B. P.; Mathijssen, S. G. J.; Wienk, M. M.; Leeuw, D. M.; Janssen, R. A. J. *J. Mater. Chem.* **2011**, *21*, 1600.

(23) Gidron, O.; Shimon, L.; Varsano, N.; Leitusw, G.; Bendikov, M. *Chem. Commun.* **2013**, *49*, 6256.

(24) (a) Zhang, L.; Colella, N. S.; Liu, F.; Trahan, S.; Baral, J. K.; Winter, H. H.; Mannsfeld, S. C. B.; Briseno, A. L. *J. Am. Chem. Soc.* **2012**, *135*, 844. (b) Izumi, T.; Kobashi, S.; Takimiya, K.; Aso, Y.; Otsubo, T. *J. Am. Chem. Soc.* **2003**, *125*, 5286. (c) Kreyenschmidt, M.; Uckert, F.; Muellen, K. *Macromolecules* **1995**, *28*, 4577. (d) Schumm, J. S.; Pearson, D. L.; Tour, J. M. *Angew. Chem., Int. Ed. Engl.* **1994**, *33*, 1360. (e) Bäuerle, P.; Fischer, T.; Bildlingmeier, B.; Stabel, A.; Rabe, J. *Angew. Chem., Int. Ed. Engl.* **1995**, *34*, 303−307.

(25) Facchetti, A.; Yoon, M.-H.; Stern, C. L.; Hutchison, G. R.; Ratner, M. A.; Marks, T. J. *J. Am. Chem. Soc.* **2004**, *126*, 13480.

(26) Cohen, E.; Bendikov, M. Unpublished results.

(27) Nakanishi, H.; Sumi, N.; Aso, Y.; Otsubo, T. *J. Org. Chem.* **1998**, *63*, 8632.

(28) The geometries of ***n*F-$_2$C$_6$** (n = 4, 6, 8) and **16F-6C$_6$** were fully optimized using the 6-31G(d) basis set (B3LYP/6-31G(d)). The optimized geometries of ***n*F-$_2$C$_6$** (n = 4, 6, 8) were further confirmed as minima by carrying out frequency calculations. All four compounds were further calculated by TD-DFT for UV and fluorescence spectra at the B3LYP/6-31G(d) level. See the Supporting Information for details.

(29) Zade, S. S.; Bendikov, M. *Org. Lett.* **2006**, *8*, 5243.

(30) All of the calculations were performed using the Gaussian 09 program. See the Supporting Information for details.

(31) Seixas de Melo, J.; Elisei, F.; Gartner, C.; Aloisi, G. G.; Becker, R. S. *J. Phys. Chem. A* **2000**, *104*, 6907.

(32) Barbarella, G.; Zambianchi, M.; Antolini, L.; Ostoja, P.; Maccagnani, P.; Bongini, A.; Marseglia, E. A.; Tedesco, E.; Gigli, G.; Cingolani, R. *J. Am. Chem. Soc.* **1999**, *121*, 8920.

(33) (a) Yang, C.; Orfino, F. P.; Holdcroft, S. *Macromolecules* **1996**, *29*, 6510. (b) Wu, Z.; Petzold, A.; Henze, T.; Thurn-Albrecht, T.; Lohwasser, R. H.; Sommer, M.; Thelakkat, M. *Macromolecules* **2010**,

43, 4646. (c) Meille, S. V.; Romita, V.; Caronna, T.; Lovinger, A. J.; Catellani, M.; Belobrzeckaja, L. *Macromolecules* **1997**, *30*, 7898.
(34) (a) Bredas, J. L.; Street, G. B. *Acc. Chem. Res.* **1985**, *18*, 309. (b) Zaikowski, L.; Kaur, P.; Gelfond, C.; Selvaggio, E.; Asaoka, S.; Wu, Q.; Chen, H.-C.; Takeda, N.; Cook, A. R.; Yang, A.; Rosanelli, J.; Miller, J. R. *J. Am. Chem. Soc.* **2012**, *134*, 10852. (c) Apperloo, J. J.; Janssen, R. A. J.; Malenfant, P. R. L.; Groenendaal, L.; Fréchet, J. M. J. *J. Am. Chem. Soc.* **2000**, *122*, 7042. (d) van Haare, J. A. E. H.; Havinga, E. E.; van Dongen, J. L. J.; Janssen, R. A. J.; Cornil, J.; Brédas, J.-L. *Chem.—Eur. J.* **1998**, *4*, 1509. (e) Apperloo, J. J.; Janssen, R. A. J.; Malenfant, P. R. L.; Fréchet, J. M. J. *J. Am. Chem. Soc.* **2001**, *123*, 6916. (f) Lin, C.; Endo, T.; Takase, M.; Iyoda, M.; Nishinaga, T. *J. Am. Chem. Soc.* **2011**, *133*, 11339.
(35) Guay, J.; Kasai, P.; Dim, A.; Wu, R. L.; Tour, J. M.; Dao, L. H. *Chem. Mater.* **1992**, *4*, 1097.
(36) Patil, A. O.; Heeger, A. J.; Wudl, F. *Chem. Rev.* **1988**, *88*, 183.
(37) Zade, S. S.; Bendikov, M. *Chem.—Eur. J.* **2008**, *14*, 6734.
(38) Eugster, N.; Fermin, D. J.; Girault, H. H. *J. Phys. Chem. B* **2002**, *106*, 3428.
(39) Sheberla, D.; Bendikov, M. Unpublished results.